Figure S1

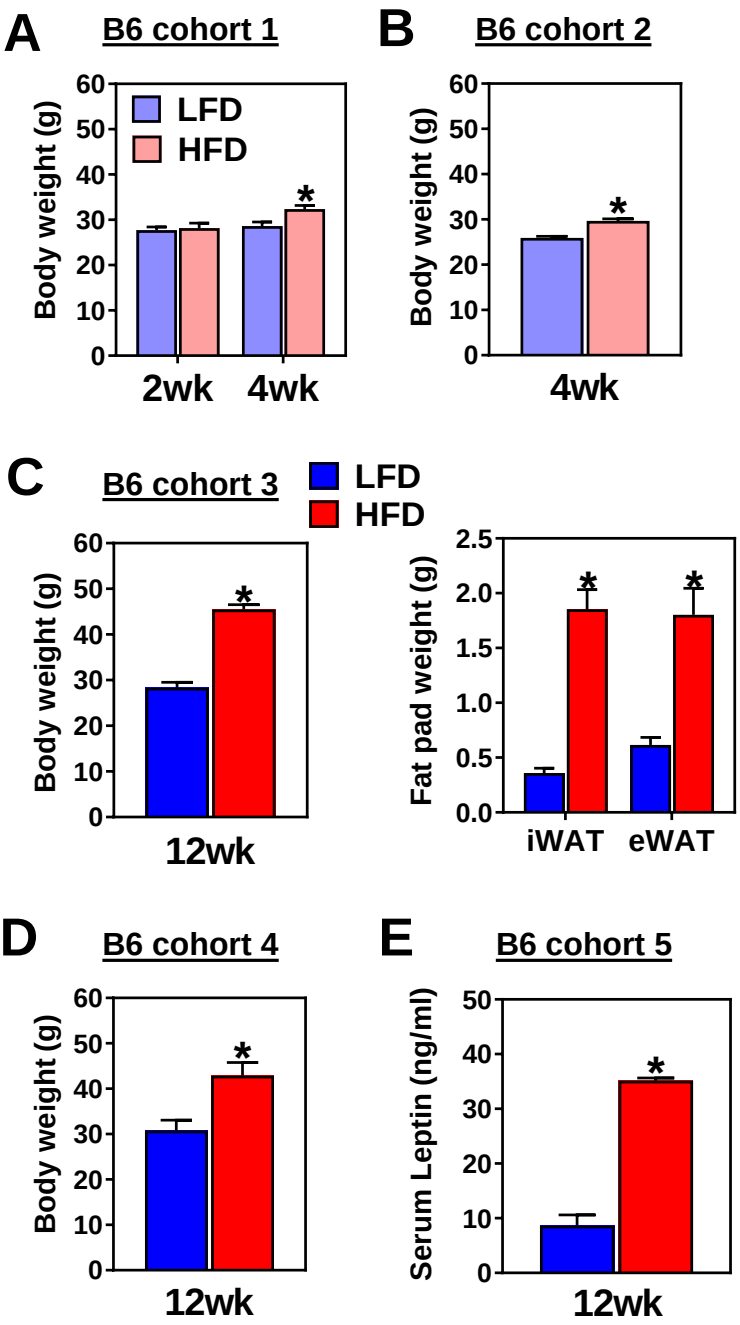

Figure S1. C57BL/6 mice develop obesity on HFD (related to Figure 1).
(A-B) Body weights of two cohorts of B6 male mice fed HFD vs LFD for 2 or 4 weeks (n=10 mice per group). (C-D) Body weights and fat pad weights for two cohorts fed these diets for 12 weeks (Cohort 3 n=5 and cohort 4 n=15 mice per group). (E) The fifth cohort was fed LFD for 12 weeks, HFD for 12 weeks, or HFD for 10 weeks followed by HFD with rosi for the final 2 weeks (n=5 mice per group). Serum leptin levels are shown here, and body weights and other measurements in this cohort are in Figures 3 and S4. (* P<0.01, T-test)

Figure S2

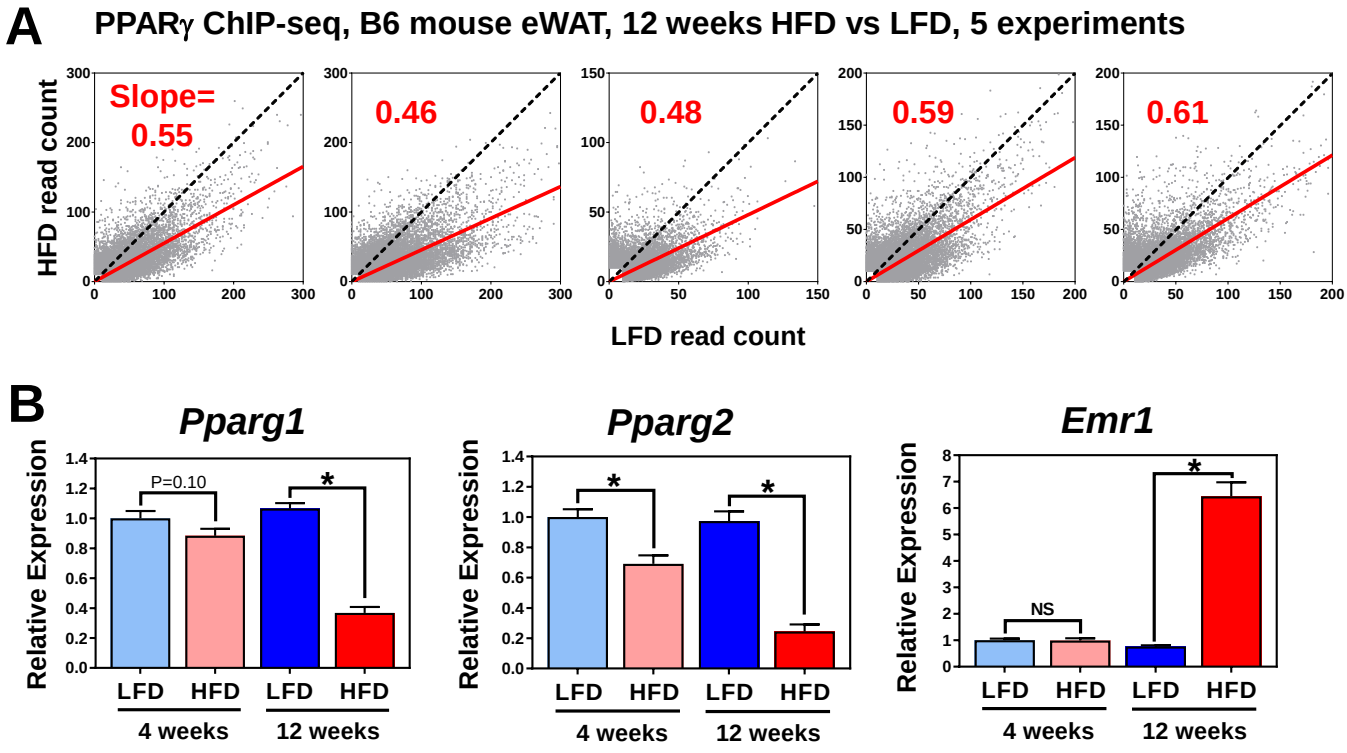

Figure S2. High fat diet decreases PPARγ expression and genome-wide occupancy in visceral fat of C57BL/6 mice (related to Figure 2). (A) Scatterplots of five independent PPARγ ChIP-seq experiments on three different mouse cohorts comparing occupancy in eWAT on HFD for 12 weeks versus control LFD. (#1-2 on cohort 4, #3 on cohort 3, #4-5 on cohort 5). The slope of linear regression (red) shows consistently less occupancy on HFD, while the dotted line shows slope of 1 or equal occupancy. (B) Quantitative RT-PCR for *Pparg1*, *Pparg2*, and the macrophage marker *Emr1*, normalized to the housekeeping control gene *Rplp0/36B4*, in B6 eWAT on HFD versus LFD for 4 or 12 weeks (* P<0.01, T-test). (C) anti-PPARγ Western Blot in eWAT on HFD versus LFD for 12 weeks, n=3 mice per diet from cohort 3.

Figure S3

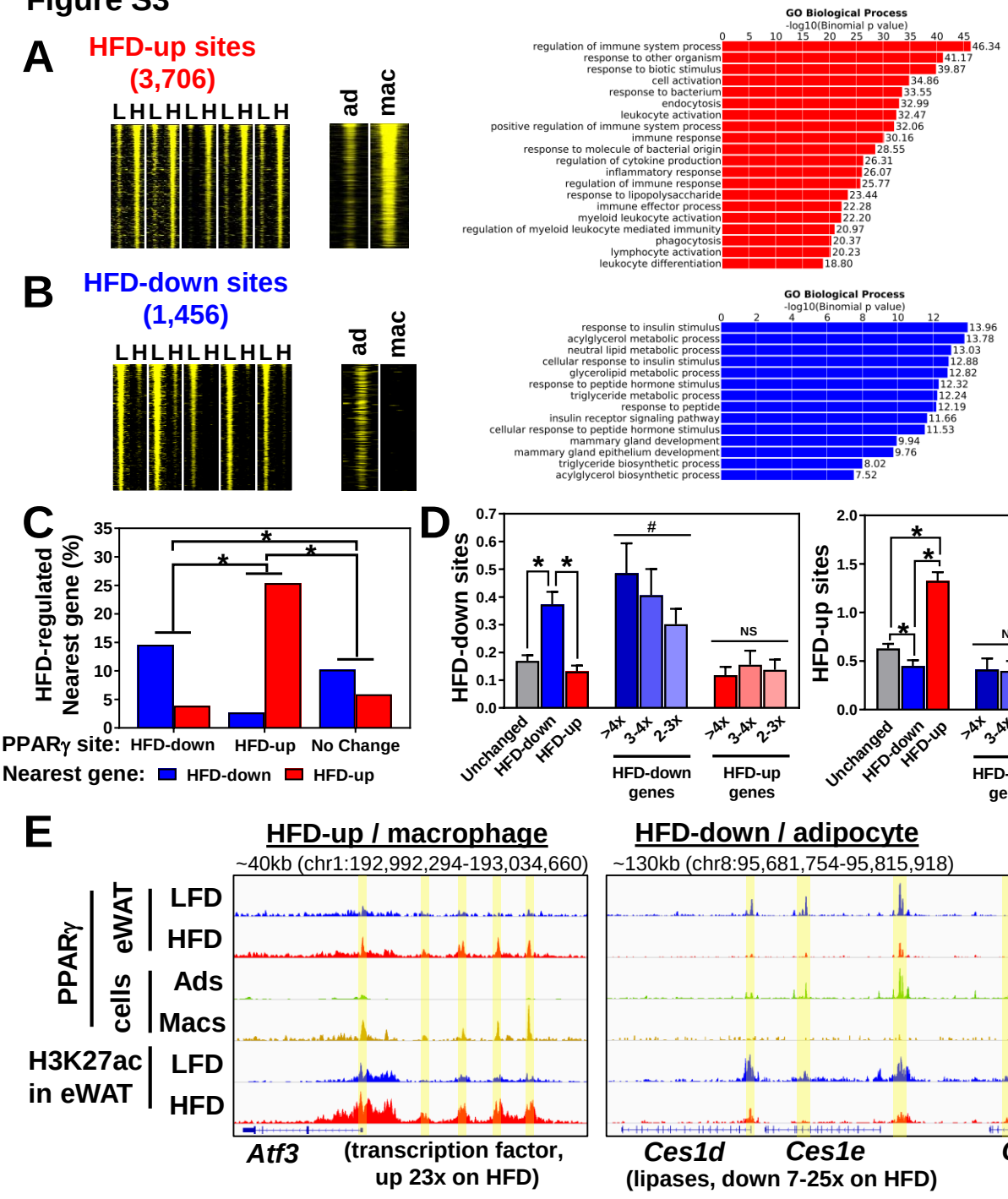

Figure S3. High fat diet alters PPARγ occupancy and gene regulation in visceral fat of C57BL/6 mice (related to Figure 2). (A) Heatmap showing HFD-up PPARγ sites consistent in 5 experiments (L=LFD, H=HFD), and enriched for macrophage (mac) selective sites. Pathway analysis (right) shows enriched immune and inflammatory processes. (B) Same for HFD-down PPARγ sites, which were also reproducible yet showed enrichment of adipocyte (ad) sites and adipocyte metabolic pathways. (C) Each PPARγ site was assigned to the nearest TSS within 100kb, HFD-down and HFD-up sites both showed enrichment of similarly regulated nearest genes (*, P<0.0001 Chi-square). (D) Genes were binned by their change on HFD and diet-regulated PPARγ sites within +/- 100kb of the TSS were counted. The degree of gene HFD down-regulation correlated with the number of nearby HFD-down sites (left), and likewise for HFD-up genes and sites (right). (*P<0.01 Mann-Whitney, #P<0.05 Kruskal-Wallis) (E) Browser track examples of a locus (left, *Atf3*) with HFD-up PPARγ occupancy in eWAT, macrophage selective PPARγ sites (yellow), and HFD-up histone acetylation, and another locus (right, *Ces1* cluster) with HFD-down PPARγ binding and histone acetylation at adipocyte-selective sites.

Figure S4

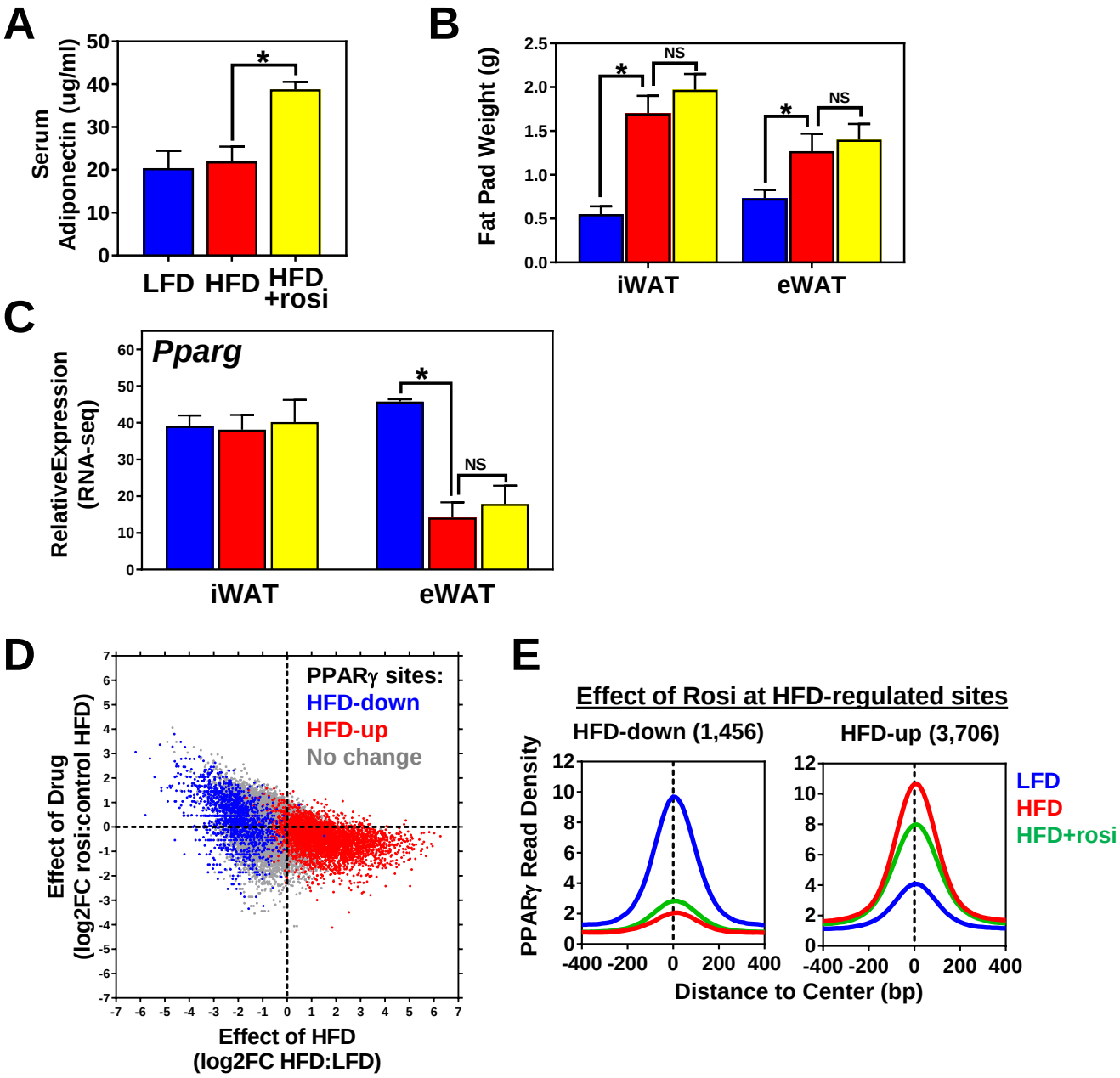

Figure S4. Effect of rosiglitazone in HFD obese C57BL/6 mice (related to Figure 3).
(A) Rosiglitazone (rosi) increased serum adiponectin levels. (B) eWAT and iWAT fat pad weights increased on HFD versus LFD, but rosi did not change them significantly. (C) PPARγ gene expression in B6 iWAT and eWAT on all three diets. (D) Scatterplot comparing the effect of HFD on each PPARγ site (down/blue or up/red dots based on Figure 2A) to the effect of the drug rosi. (E) Average profiles of PPARγ binding at HFD-down and HFD-up sites identified in Figure 2A, showing the effects of LFD versus HFD versus HFD with rosi. (* P<0.01, T-test).

Figure S5

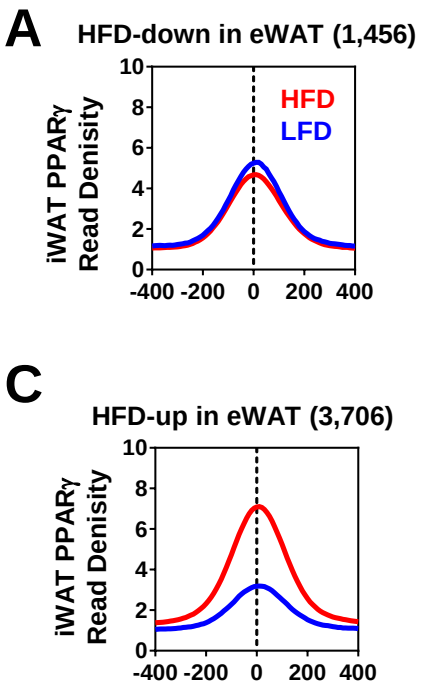

E

PANTHER Biological Process (P-value)

Cell cycle	1.26E-09
Mitosis	3.91E-08
Chromosome segregation	2.16E-05

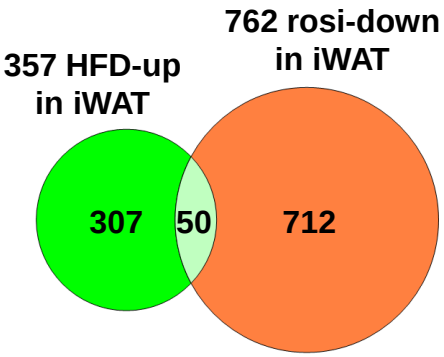

PANTHER Biological Process (P-value)

Cell structure and motility	2.64E-13
Cell adhesion	4.28E-13
Cell adhesion-mediated signaling	7.68E-11
Cell motility	4.08E-10
Cell communication	2.99E-09
Signal transduction	2.09E-06
Receptor protein tyrosine kinase signaling pathway	2.67E-06
Developmental processes	1.53E-05
Extracellular matrix protein-mediated signaling	2.09E-05
Protein phosphorylation	6.03E-05
Mesoderm development	8.85E-05

Figure S5. Effects of HFD and rosiglitazone in iWAT of C57BL/6 mice (related to Figure 3).
(A) HFD-down adipocyte PPARγ sites identified in eWAT (from Figure 2D) showed little change in average profile in iWAT on HFD. (B) Venn diagram showing HFD-down genes identified in eWAT (from Figure 1A) showed little overlap with HFD-down genes in iWAT. (C) HFD-up macrophage PPARγ sites identified in eWAT (from Figure 2C) showed a similar increase in average profile in iWAT on HFD. (D) Venn diagram showing that HFD-up genes identified in eWAT (from Figure 1A) had good overlap with HFD-up genes in iWAT, though the degree of regulation was more in eWAT. (E) Venn diagram showing that genes HFD-up in iWAT (from previous panel) were not the same genes that were rosi down-regulated in iWAT (from Figure 3D), and these genes reflect different biological pathways.

Figure S6

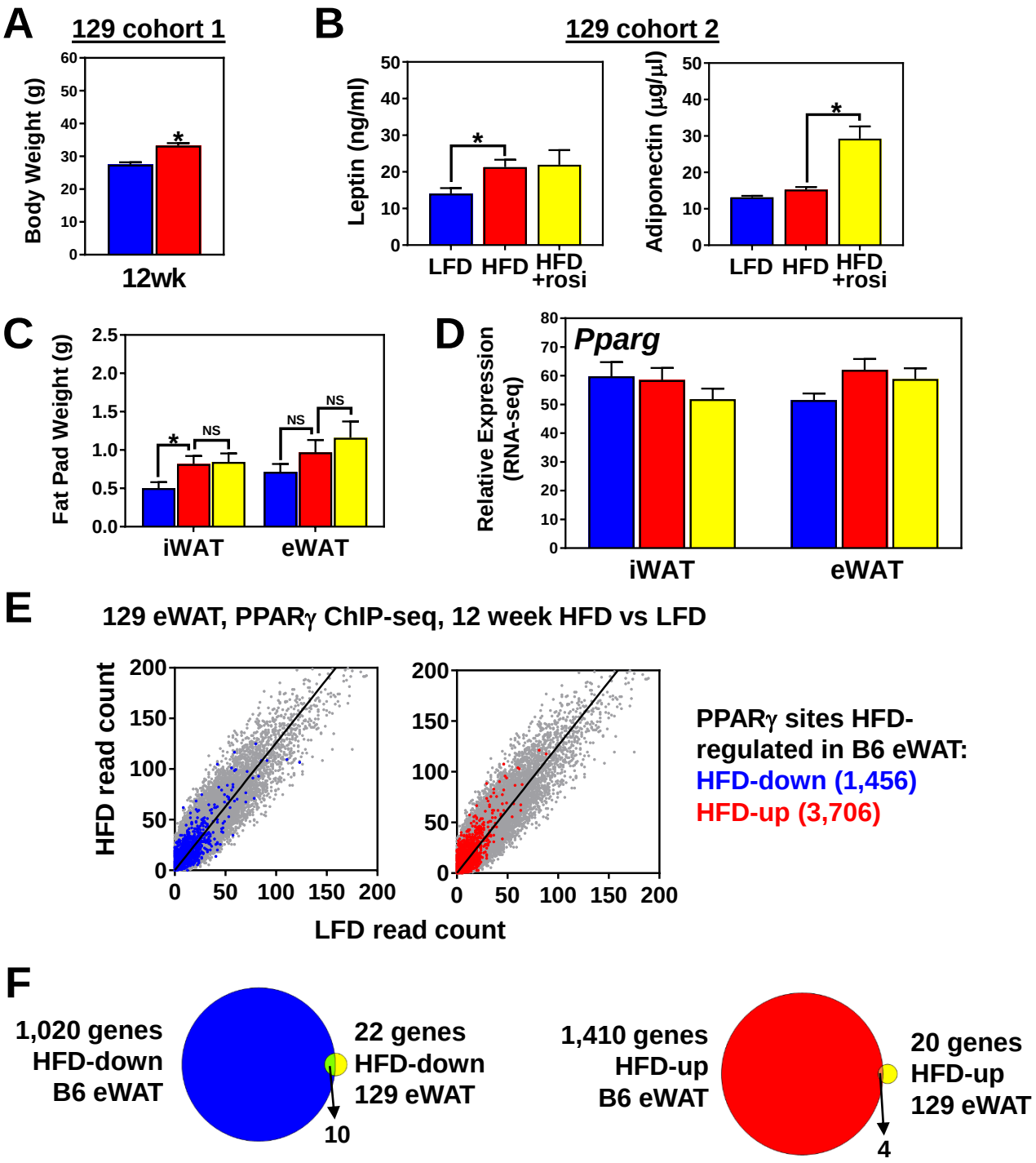

Figure S6. 129S1/SvImJ mice respond less to HFD than C57BL/6J mice (related to Figure 4).
Two cohorts of 129 mice were fed HFD versus LFD for 12 weeks. (A) Body weights of cohort 1 (n=10 mice per group). (B-C) Cohort 2 also included a HFD+rosi arm (n=5 mice per group). Serum leptin and adiponectin levels and fat pad weight are here, while body weights and other measurements in this cohort are in Figure 4. (D) PPARγ gene expression in 129 iWAT and eWAT on all three diets. (E) Scatterplot of PPARγ ChIP-seq data from 129 eWAT on HFD versus LFD. The sites previously identified in B6 eWAT (Figure 2A) as HFD-down (left, blue) and HFD-up (right, red) show no major effect of diet in 129 eWAT. (F) Venn diagrams comparing the very few HFD-regulated genes in 129 eWAT (yellow) with the many HFD-down (blue) and HFD-up (red) genes identified in B6 eWAT in Figure 1A.

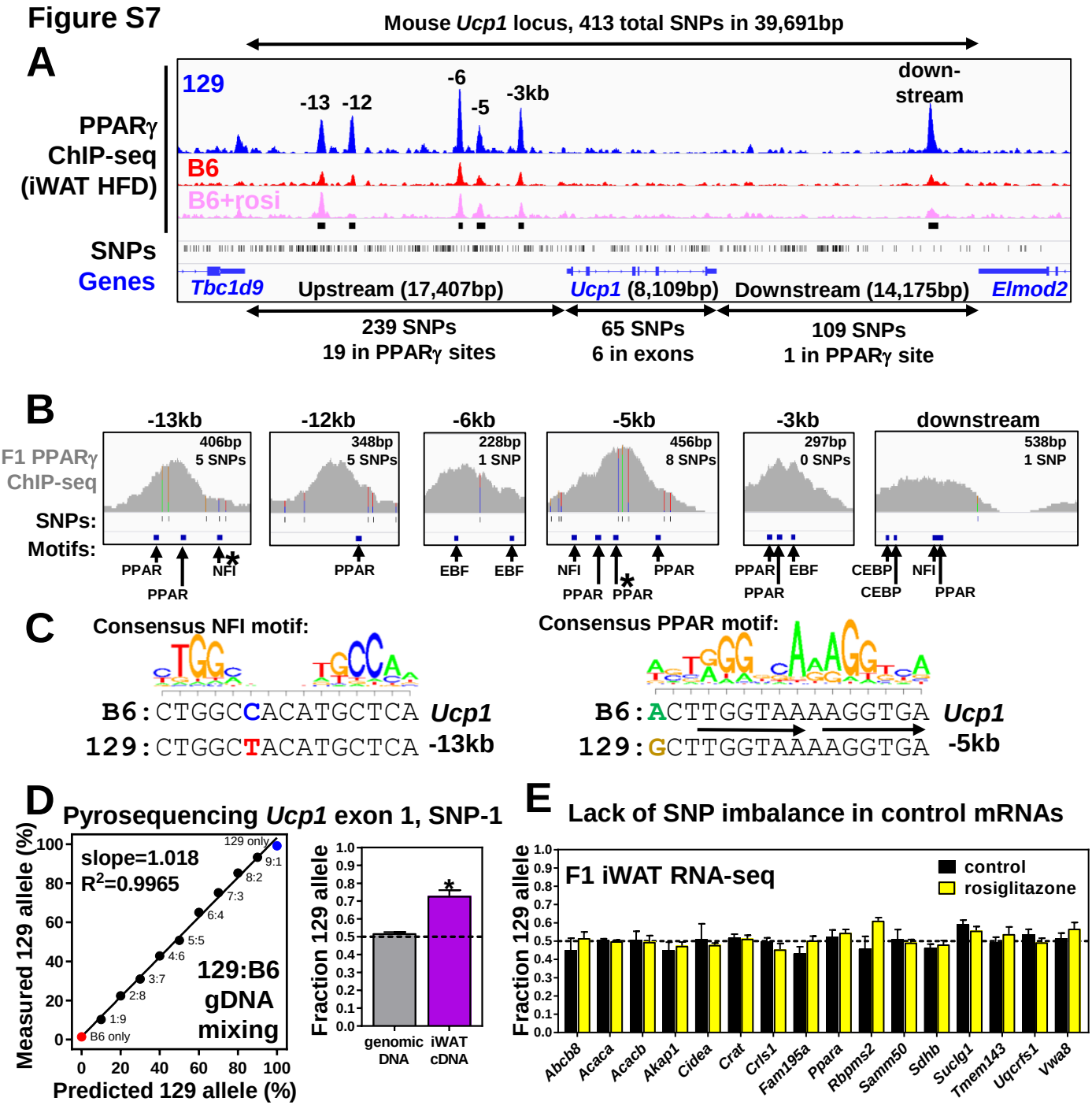

Figure S7. Imbalanced PPARγ occupancy and mRNA expression of *Ucp1* in iWAT favoring 129 over B6, but not other similarly regulated genes. (A) Genome browser view of ~40kb *Ucp1* locus showing all SNPs differing between B6 and 129 mice. PPARγ ChIP-seq shows more binding in 129 than B6 iWAT, but that rosiglitazone does not change occupancy. (B) For each of the six PPARγ binding regions, SNPs and transcription factor motifs (PPAR, CEBP, NFI, and EBF) were identified, and only two SNPs fall in motifs (starred). (C) Neither motif SNP shows a large allelic difference in consensus agreement, and both slightly favor B6 - while binding favors 129. (D) In the left panel, genomic DNA from B6 and 129 mice was mixed at the indicated ratios and subjected to pyrosequencing to measure allelic representation in each mixture. The predicted and measured values showed a tight and linear correlation. In the right panel, F1 mouse genomic DNA showed equal representation of the B6 and 129 alleles as expected, yet cDNA from iWAT favored the 129 alleles (* P<0.01, T-test). (E) 16 genes showed similar regulation to *Ucp1* and have exonic B6:129 SNPs to measure imbalance in F1 iWAT (see Table S3). Based on RNA-seq reads, none showed imbalanced expression in F1 iWAT in the presence or absence of rosi (in contrast to *Ucp1* in Figure 7A-B).